

A Mathematical Motivation for Complex-valued Convolutional Networks

Joan Bruna, Soumith Chintala, Yann LeCun, Serkan Piantino, Arthur Szlam, Mark Tygert

Facebook Artificial Intelligence Research, 1 Facebook Way, Menlo Park, California 94025

Keywords: deep learning, neural networks, harmonic analysis

Abstract:

A complex-valued convolutional network (convnet) implements the repeated application of the following composition of three operations, recursively applying the composition to an input vector of nonnegative real numbers: (1) convolution with complex-valued vectors followed by (2) taking the absolute value of every entry of the resulting vectors followed by (3) local averaging. For processing real-valued random vectors, complex-valued convnets can be viewed as “data-driven multiscale windowed power spectra,” “data-driven multiscale windowed absolute spectra,” “data-driven multiwavelet absolute values,” or (in their most general configuration) “data-driven nonlinear multiwavelet packets.” Indeed, complex-valued convnets can calculate multiscale windowed spectra when the convnet filters are windowed complex-valued exponentials. Standard real-valued convnets, using rectified linear units (ReLU), sigmoidal (for example, logistic or tanh) nonlinearities, max. pooling, etc., do not obviously exhibit the same exact correspondence with data-driven wavelets (whereas for complex-valued convnets, the correspondence is much more than just a vague analogy). Courtesy of the exact correspondence, the remarkably rich and rigorous body of mathematical analysis for wavelets applies directly to (complex-valued) convnets.

1 Introduction

Convolutional networks (convnets) have become increasingly important to artificial intelligence in recent years, as reviewed by LeCun et al. (2015). The present paper presents a theoretical argument for complex-valued convnets and their remarkable performance; complex-valued convnets turn out to calculate “data-driven multiscale windowed spectra” characterizing certain stochastic processes common in the modeling of time series (such as audio) and natural images (including patterns and textures). We motivate the construction of such multiscale spectra via “local averages of multiwavelet absolute values” or, more generally, “nonlinear multiwavelet packets.”

A textbook treatment of all concepts and terms used above and below is given by Mallat (2008). Further information is available in the original work of Daubechies (1992), Meyer (1993), Coifman et al. (1994), Coifman and Donoho (1995), Simoncelli and Freeman (1995), Meyer and Coifman (1997), LeCun et al. (1998), Donoho et al. (2003), Srivastava et al. (2003), Rabiner and Schafer (2007), and Mallat (2008), for example. The work of Haensch and Hellwich (2010), Mallat (2010), Poggio et al. (2012), Bruna and Mallat (2013), Bruna et al. (2015), and Chintala et al. (2015) also develops complex-valued convnets, providing copious applications and numerical experiments. A related, more sophisticated connection (to renormalization group theory) is given by Mehta and Schwab (2014). Our exposition relies on nothing but the basic signal processing treated by Mallat (2008). Via the connections discussed below, the rich, rigorous mathematical analysis surveyed by Daubechies (1992), Meyer (1993), Mallat (2008), and others applies directly to complex-valued convnets.

Citing such connections, the present paper’s anonymous reviews suggested viewing complex-valued convnets as a kind of baseline architecture for much of the deep learning reviewed by LeCun et al. (2015). Section 6 presents numerical analyses corroborating this viewpoint. Having such a theoretical basis for deep learning could help in paring down the combinatorial explosion of possibilities for future developments, while probably also illuminating further possibilities.

The present paper proceeds as follows: Section 2 reviews stationary stochastic processes and their spectra. Section 3 reviews locally stationary stochastic processes and the connection of their spectra to stages in a complex-valued convnet. Section 4 introduces multiscale (multiple stages in a convnet). Section 5 describes the fitting/learning/training that the connection to convnets facilitates. Section 6 briefly compares on a common benchmark the accuracies for the complex-valued convnets of Chintala et al. (2015) to those for the scattering transforms of Mallat (2010) and for the standard real-valued convnets of Krizhevsky et al. (2012). Section 7 generalizes and summarizes the aforementioned sections.

2 Stationary stochastic processes

For simplicity, we first limit consideration to the special case of a doubly infinite sequence of nonnegative random variables X_k , where k ranges over the integers. This input data will be the result of convolving an unmeasured independent and identically distributed (i.i.d.) sequence Z_k , where k ranges over the integers, with an unknown sequence of real numbers f_k , where k ranges over the integers (this latter sequence is known as a “filter,” whereas the i.i.d. sequence is known as “white noise”):

$$X_j = \sum_{k=-\infty}^{\infty} f_{j-k} Z_k \quad (1)$$

for any integer j . Such a sequence X_k , with k ranging over the integers, is a (strictly) “stationary stochastic process.” The terminology “strictly stationary” refers to the fact that lagging or shifting the process preserves the probability distribution of the process: indeed, for any integer l , the shift $Y_k = X_{k-l}$, where k ranges over the integers, satisfies

$$Y_j = \sum_{k=-\infty}^{\infty} f_{j-k} Z'_k \quad (2)$$

for any integer j , where $Z'_k = Z_{k-l}$; the sequence Z'_k , with k ranging over the integers, is i.i.d. with the same distribution as Z_k , where k ranges over the integers.

The associated “absolute spectrum” is

$$\tilde{X}(\omega) = \lim_{n \rightarrow \infty} \mathbf{E} \left| \frac{1}{\sqrt{2n+1}} \sum_{k=-n}^n e^{-ik\omega} X_k \right| \quad (3)$$

for any real number ω (usually we consider not just any, but instead restrict consideration to a sequence running from 0 to about 2π). Please note that lagging or shifting the process changes neither the probability distribution of the process (since the process is stationary) nor the absolute spectrum: for any integer l , the shift $Y_k = X_{k-l}$ yields $\tilde{Y}(\omega) = \tilde{X}(\omega)$ for any real number ω , due to the absolute value in equation 3.

Similarly, the associated “power spectrum” is

$$\tilde{\tilde{X}}(\omega) = \lim_{n \rightarrow \infty} \mathbf{E} \left(\left| \frac{1}{\sqrt{2n+1}} \sum_{k=-n}^n e^{-ik\omega} X_k \right|^2 \right) \quad (4)$$

for any real number ω ; there is an extra squaring under the expectation in equation 4 compared to equation 3. Again, lagging or shifting the process changes neither the probability distribution of the process nor the power spectrum: for any integer l , the shift $Y_k = X_{k-l}$ yields $\tilde{Y}(\omega) = \tilde{X}(\omega)$ for any real number ω , due to the absolute value in equation 4. The remainder of the present paper focuses on the absolute spectrum; most of the discussion applies to the power spectrum, too.

Remark 1. The absolute spectrum can be more robust than the power spectrum, in the same sense that the mean absolute deviation can be more robust than the variance or standard deviation. The power spectrum is more fundamental in a certain sense, yet the absolute spectrum may be preferable for applications to machine learning. We conjecture that both can work about the same. We focus on the absolute spectrum to simplify the exposition.

3 Locally stationary stochastic processes

In practice, the input data is seldom strictly stationary, but usually only locally stationary, that is, equation 1 becomes

$$X_j = \sum_{k=-\infty}^{\infty} f_{j-k}^{(j)} Z_k \quad (5)$$

for any integer j , where $f_k^{(j)}$ changes much more slowly when changing j than when changing k . To accommodate such data, we introduce windowed spectra; for any even nonnegative-valued sequence g_k , with k ranging through the integers — this sequence could be samples of a Gaussian or any other window suitable for Gabor analysis (the data itself will determine g during training) — we consider

$$\tilde{X}_l(\omega) = \frac{1}{2n+1} \sum_{j=-n+l}^{n+l} \left| \frac{1}{\sqrt{2n+1}} \sum_{k=-\infty}^{\infty} e^{-ik\omega} g_{k-j} X_k \right| \quad (6)$$

for any integer l , with some positive integer n . The extra summation in equation 6 averages away noise and is a kind of approximation to the expected value in equation 3. Usually g_k is fairly close to 1 for $k = -n, -n+1, \dots, n-1, n$, and g_k is fairly close to 0 for $|k| > n$, making a reasonably smooth transition between 0 and 1. The most important difference between equation 3 and equation 6 is the absence of a limit in the latter (hence the terminology, “local” spectrum).

Due to the absolute value, equation 6 is equivalent to

$$\tilde{X}_l(\omega) = \frac{1}{2n+1} \sum_{j=-n+l}^{n+l} \left| \frac{1}{\sqrt{2n+1}} \sum_{k=-\infty}^{\infty} g_{j-k}(\omega) X_k \right| \quad (7)$$

for any *even* nonnegative-valued sequence g_k , with k ranging through the integers, where

$$g_k(\omega) = e^{ik\omega} g_k \quad (8)$$

for any integer k (“even” means that $g_{-k} = g_k$ for every integer k). Please note that the right-hand side of equation 7 is just a convolution followed by the absolute value followed by local averaging; this will facilitate fitting/learning/training using data — enabling a “data-driven” approach — in Section 5.

4 Multiscale

In most cases, the ideal choices of n and width of the window in equation 7, that is, the ideal number of indices for which g_k is substantially nonzero, are far from obvious. Often, in fact, multiple widths are relevant (say, wider for lower-frequency variations than for higher frequency). Not knowing the ideal a priori, we use multiple windows on multiple scales. An especially efficient multiscale implementation processes the results of the lowest-frequency channels recursively. For the lowest frequency, $\omega = 0$, and when X_k is nonnegative for every integer k (for example, the input X_k could be the \tilde{X}_k arising from previous processing), equation 7 simplifies to

$$\tilde{X}_l(0) = \frac{1}{\sqrt{2n+1}} \sum_{k=-\infty}^{\infty} h_{l-k} X_k \quad (9)$$

for any integer l , where

$$h_l = \frac{1}{2n+1} \sum_{j=-n+l}^{n+l} g_j \quad (10)$$

for any integer l , and again g_j , with j ranging through the integers, is an even sequence of non-negative real numbers (“even” means that $g_{-j} = g_j$ for every integer j). The result of equation 9 is simply a convolution with the input sequence, and further convolutions — say via recursive processing of the form in equation 7 — can undo this convolution and set the effective window however desired in later stages. The deconvolution and subsequent convolution with the windowed exponential of a later stage is numerically stable if the later window is wider than the preceding. In particular, recursively processing the zero-frequency channels in this way can implement a “wavelet transform” (if each recursive stage considers only two values for ω , one zero and one nonzero — see Figure 1) or a “multiwavelet transform” (if each recursive stage considers multiple values for ω , with one of the values being zero — see Figure 2). For multidimensional signals, multiwavelets detect local directionality beyond what wavelets provide. If we recursively process the higher-frequency channels, too, then we obtain a “nonlinear wavelet packet transform” or a “nonlinear multiwavelet packet transform” — a kind of nonlinear iterated filter bank — see Figure 3. Linearly recombining the different frequency channels may help realize local rotation-invariance and other potentially desirable properties (indeed, Mallat (2010) did this for rotations and other transformations) — including generating harmonics when processing audio signals. The transforms just discussed are undecimated, but interleaving appropriate decimation or subsampling applied to the sequences yields the usual decimated transforms.

Remark 2. In practice, decimation or subsampling is important to avoid overfitting in the data-driven approach discussed below, by limiting the number of degrees of freedom appropriately. Even when the signal is not a strictly stationary stochastic process, the averaging in equation 7 — the leftmost summation — performs the “cycle spinning” of Coifman and Donoho (1995) to avoid artifacts that would otherwise arise due to windows’ partitioning after subsampling. The averaging reduces the variance; wider averaging would further reduce the variance.

Remark 3. Sequences that are finite rather than doubly infinite provide only enough information for estimating a smoothed version of the spectrum. Alternatively, a finite amount of data provides information for estimating multiscale windowed spectra yielding time-frequency (or space-Fourier) resolution similar to the multiresolution analysis of wavelets.

Remark 4. SIFT, HOG, SURF, etc. of Lowe (1999), Lowe (2004), Dalal and Triggs (2005), Bay et al. (2008), and others are more analogous to the multiwavelet architecture of Figure 2 than to the more general wavelet-packet architecture of Figure 3.

5 Fitting/learning/training

The “multiwavelet transform” constitutes a desirable baseline model. We can easily adapt to the data the choices of windows and indeed the whole recursive structure of the processing (whether restricting the recursion to the zero-frequency channels, or also allowing the recursive processing of higher-frequency channels). Viewing the convolutional filters in equation 7 that serve as windowed exponentials as parameters, the desirable baseline is just one member of a parametric family of models. This parametric family is known as a “complex-valued convolutional network.” We can fit (that is, learn or train) the parameters to the data via optimization procedures such as stochastic gradient descent in conjunction with “backpropagation” (backpropagation is the chain rule of Calculus applied to calculate gradients of our recursively composed operations). For “supervised learning,” we optimize according to a specified objective, usually using the multiscale spectra as inputs to a scheme for classification or regression, as detailed by LeCun et al. (1998), for example.

Remark 5. In consonance with the “best-basis” approach of Coifman et al. (1994) and Saito and Coifman (1995), a potentially more efficient possibility is to restrict the convolutional filters in equation 7 to be windowed exponentials that are designed completely a priori, aside from one overall scaling factor per filter, fitting/learning/training only the scaling factors. How best to effect this approach is an open question.

6 Numerical experiments

The following reports the classification accuracies for the complex-valued convnets of Chintala et al. (2015), the standard real-valued convnets of Krizhevsky et al. (2012), and the scattering transforms of Oyallon and Mallat (2015), on a benchmark data set, “CIFAR-10,” from Krizhevsky (2009) (CIFAR-10 contains 50,000 images in its training set and 10,000 images in its testing set; each image falls into one of ten classes, is full-color, and consists of a 32×32 grid of pixels): According to Table 4 of Oyallon and Mallat (2015), the scattering transforms attain an error rate of 18% on the test set, after training their classifiers on the training set. According to Section 3.3 of Krizhevsky et al. (2012), a standard real-valued convnet attains an error rate of 13% on the test set without the “local response normalization” of that Section 3.3, and attains 11% with the local response normalization. The complex-valued convnets detailed in Chintala et al. (2015) attain an error rate of 12% on the test set, at least when using a larger net and training with enough iterations for the test error to settle down and converge (for complex-valued convnets, accuracy seems to improve as the net becomes larger — for the error rate of 12%, a net eight times the size of that reported in Table 1 of Chintala et al. (2015) was sufficient, using the same kernel sizes and other parameter settings as for Table 1). Augmenting the training images with their mirror images improved convergence to the reported accuracies. All in all, the extensively trained real- and complex-valued convnets yielded similar error rates, which are about a third less than those which scattering transforms attained. Of course, the fitting/learning/training involved for classification with the scattering transforms is much less extensive.

7 Conclusion

While the above concerns X_k , where k ranges over the integers, extension to analyzing $X_{j,k}$, where j and k range over the integers, is straightforward — the latter could be a “locally homogeneous random field.” Also, the infinite range of the integers is far from essential; implementations on computers obviously use only finite sequences. Moreover, the above construction is appropriate

for processing any locally stationary stochastic process, not just filtered white noise. For instance, the construction can enable a multiresolution analysis of “regularity” (or “smoothness”) that easily distinguishes between low-pass filtered i.i.d. Gaussian noise and a pulse train or sinusoid with a random phase offset (for example, $X_k = 1 + \sin(\pi(k + J)/1000)$ for any integer k , where J is an integer drawn uniformly at random from $1, 2, \dots, 2000$). More generally, the construction should enable discriminating between many interesting classes of stochastic processes, commensurate with the ability of multiwavelet-based multiresolution analysis to measure “regularity,” “intermittency,” distributional characteristics (say, Gaussian versus Poisson), etc. Any globally stationary stochastic process — with or without intermittent fluctuations — can be modeled as above as a locally stationary stochastic process (of course, Bruna et al. (2015) treat the former directly, to great advantage in the analysis of homogeneous turbulence and other phenomena from statistical physics). Every model in the parametric family constituting the complex-valued convnet calculates relevant features, windowed spectra of the form in equation 6 and equation 7. The absolute values in equation 6 and equation 7 are the key nonlinearity, a reflection of the local stationarity — the local translation-invariance — of the process and its relevant features.

Acknowledgments

We would like to thank Keith Adams, Lubomir Bourdev, Rob Fergus, Armand Joulin, Manohar Paluri, Christian Puhersch, Marc’Aurelio Ranzato, Ben Recht, and Rachel Ward.

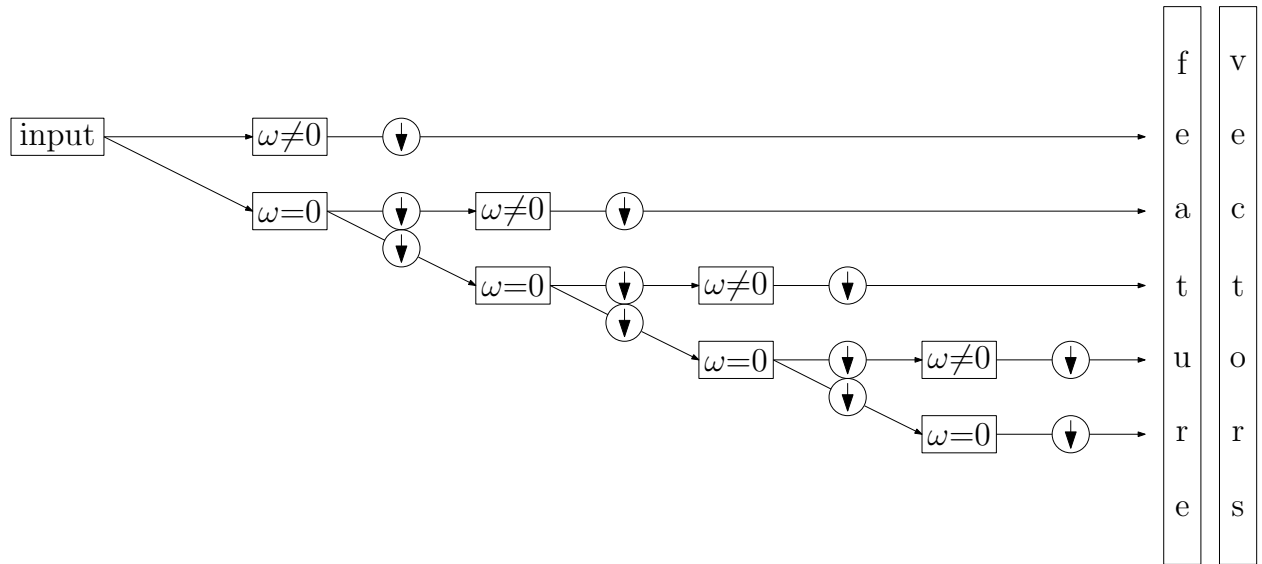


Figure 1: A flow chart for the “wavelet transform” of an input vector: each box “ $\omega=0$ ” corresponds to equation 7 with $\omega=0$ or (equivalently) to equation 9; each box “ $\omega\neq0$ ” corresponds to equation 7 — convolution followed by taking the absolute value of every entry followed by local averaging; each circle “ \downarrow ” corresponds to subsampling (say, retaining only every other entry)

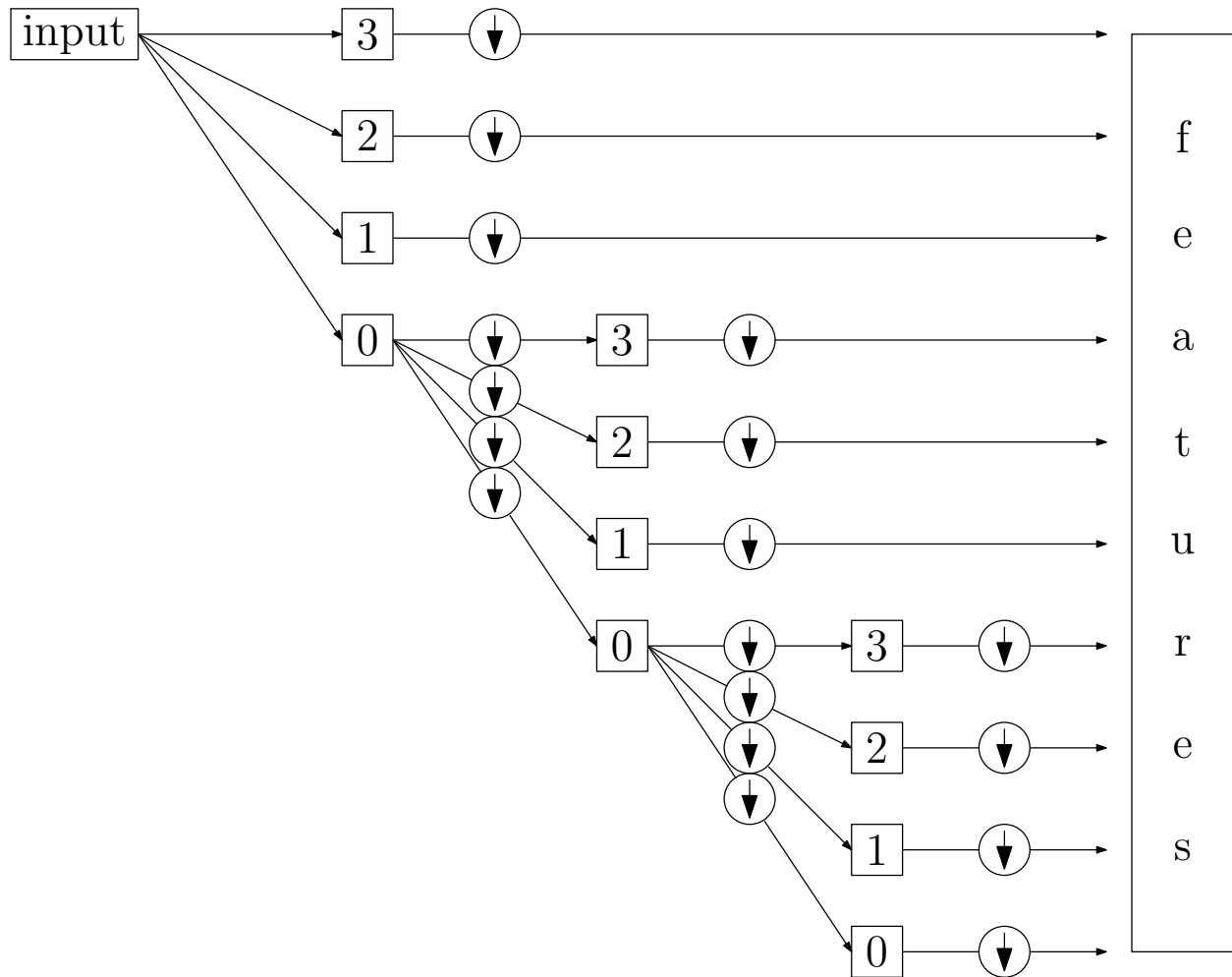


Figure 2: A flow chart for the “multiwavelet transform” of an input vector: each box “0” corresponds to equation 7 with $\omega=0$ or (equivalently) to equation 9; each box “1,” “2,” or “3” corresponds to equation 7 for different convolutional filters, but always with convolution followed by taking the absolute value of every entry followed by local averaging; each circle “ \downarrow ” corresponds to subsampling (say, retaining only every fourth entry)

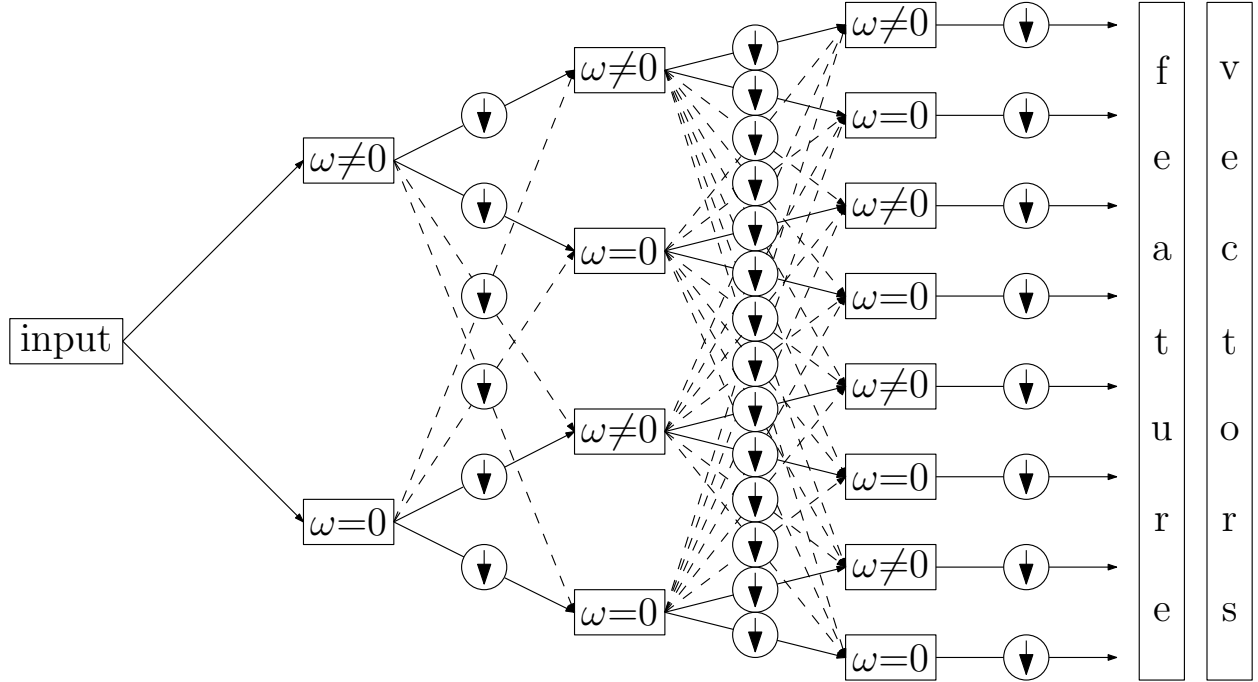


Figure 3: A flow chart for the “nonlinear wavelet packet transform” of an input vector: each box “ $\omega=0$ ” corresponds to equation 7 with $\omega=0$ or (equivalently) to equation 9; each box “ $\omega\neq0$ ” corresponds to equation 7 — convolution followed by taking the absolute value of every entry followed by local averaging; each circle “ \downarrow ” corresponds to subsampling (say, retaining only every other entry); the dashed arrows can involve downweighting the associated summands (and the convolutional filter can be different for every arrow); Figure 1 is essentially a special case of the present figure for which some of the convolutional filters simply deconvolve the preceding local averaging (omitting some of the subsampling)

References

- Bay, H., Ess, A., Tuytelaars, T., and Gool, L. V. (2008). Speeded-up robust features (SURF). *Computer Vision Image Understanding*, 110(3):346–359.
- Bruna, J. and Mallat, S. (2013). Invariant scattering convolutional networks. *IEEE Trans. Pattern Analysis Machine Intel.*, 35(8):1872–1886.
- Bruna, J., Mallat, S., Bacry, E., and Muzy, J.-F. (2015). Intermittent process analysis with scattering moments. *Ann. Statist.*, 43(1):323–351.
- Chintala, S., Ranzato, M., Szlam, A., Tian, Y., Tygert, M., and Zaremba, W. (2015). Scale-invariant learning and convolutional networks. Technical Report 1506.08230, arXiv.
- Coifman, R. R. and Donoho, D. (1995). Translation-invariant denoising. In Antoniadis, A. and Oppenheim, G., editors, *Wavelets and Statistics*, volume 103 of *Lecture Notes in Statistics*, pages 125–150. Springer.
- Coifman, R. R., Meyer, Y., Quake, S., and Wickerhauser, M. V. (1994). Signal processing and compression with wavelet packets. In Byrnes, J. S., Byrnes, J. L., Hargreaves, K. A., and Berry, K., editors, *Wavelets and Their Applications*, volume 442 of *NATO ASI Series C: Mathematical and Physical Sciences*, pages 363–379. Springer.
- Dalal, N. and Triggs, B. (2005). Histograms of oriented gradients for human detection. In *IEEE Computer Society Conf. Computer Vision and Pattern Recognition 2005*, volume 1, pages 886–893. IEEE.
- Daubechies, I. (1992). *Ten Lectures on Wavelets*. CBMS-NSF Regional Conference Series in Applied Mathematics. SIAM.
- Donoho, D., Mallat, S., von Sachs, R., and Samuelides, Y. (2003). Locally stationary covariance and signal estimation with macrotiles. *IEEE Trans. Signal Processing*, 51(3):614–627.
- Haensch, R. and Hellwich, O. (2010). Complex-valued convolutional neural networks for object detection in PolSAR data. In *8th European Conf. EUSAR*, pages 1–4. IEEE.
- Krizhevsky, A. (2009). Learning multiple layers of features from tiny images. Technical Report Master’s Thesis, University of Toronto Department of Computer Science.
- Krizhevsky, A., Sutskever, I., and Hinton, G. (2012). ImageNet classification with deep convolutional neural networks. In *Advances in Neural Information Processing Systems*, pages 1097–1105. Curran Associates.
- LeCun, Y., Bengio, Y., and Hinton, G. (2015). Deep learning. *Nature*, 521(7553):436–444.
- LeCun, Y., Bottou, L., Bengio, Y., and Haffner, P. (1998). Gradient-based learning applied to document recognition. *Proc. IEEE*, 86(11):2278–2324.
- Lowe, D. G. (1999). Object recognition from local scale-invariant features. In *Proc. 7th IEEE Internat. Conf. Computer Vision*, volume 2, pages 1150–1157. IEEE.
- Lowe, D. G. (2004). Distinctive image features from scale-invariant keypoints. *Internat. J. Computer Vision*, 60(2):91–110.

- Mallat, S. (2008). *A Wavelet Tour of Signal Processing: the Sparse Way*. Academic Press, 3rd edition.
- Mallat, S. (2010). Recursive interferometric representations. In *Proc. EUSIPCO Conf. 2010*, pages 716–720. EURASIP.
- Mehata, P. and Schwab, D. J. (2014). An exact mapping between the variational renormalization group and deep learning. Technical Report 1410.3831, arXiv.
- Meyer, Y. (1993). *Wavelets and Operators*, volume 37 of *Cambridge Studies in Advanced Mathematics*. Cambridge University Press.
- Meyer, Y. and Coifman, R. R. (1997). *Wavelets: Calderón-Zygmund and Multilinear Operators*, volume 48 of *Cambridge Studies in Advanced Mathematics*. Cambridge University Press.
- Oyallon, E. and Mallat, S. (2015). Deep roto-translation scattering for object classification. In *IEEE Computer Society Conf. Computer Vision and Pattern Recognition 2015*, volume 1, pages 2865–2873. IEEE.
- Poggio, T., Mutch, J., Leibo, J., Rosasco, L., and Tacchetti, A. (2012). The computational magic of the ventral stream: sketch of a theory (and why some deep architectures work). Technical Report MIT-CSAIL-TR-2012-035, MIT CSAIL, Cambridge, MA.
- Rabiner, L. R. and Schafer, R. W. (2007). *Introduction to Digital Speech Processing*, volume 1 of *Foundations and Trends in Signal Processing*. NOW.
- Saito, N. and Coifman, R. R. (1995). Local discriminant bases and their applications. *J. Math. Imaging Vision*, 5(4):337–358.
- Simoncelli, E. P. and Freeman, W. T. (1995). The steerable pyramid: a flexible architecture for multi-scale derivative computation. In *Proc. Internat. Conf. Image Processing 1995*, volume 3, pages 444–447. IEEE.
- Srivastava, A., Lee, A. B., Simoncelli, E. P., and Zhu, S. (2003). On advances in statistical modeling of natural images. *J. Math. Imaging Vision*, 18(1):17–33.